**Monograph:**
Li, L.M. and Billings, S.A. (2010) Piecewise Volterra modelling of the Duffing oscillator in the frequency domain. Research Report. ACSE Research Report no. 1015 . Automatic Control and Systems Engineering, University of Sheffield

# Piecewise Volterra modelling of the Duffing oscillator in the frequency domain

**L.M.Li and S.A.Billings**

**Department of Automatic Control**
**and Systems Engineering,**
**University of Sheffield, Sheffield**
**Post Box 600 S1 3JD**
**UK**

**Research Report No. 1015**

**September 2010**

# Piecewise Volterra modelling of the Duffing oscillator in the frequency domain

L. M. Li and S. A. Billings

Department of Automatic Control and Systems Engineering
University of Sheffield
Sheffield S1 3JD
UK
*S.Billings@sheffield.ac.uk

**Abstract:** When analysing the nonlinear Duffing oscillator, the weak nonlinearity is basically dependent on the amplitude range of the input excitation. The nonlinear differential equation models of such nonlinear oscillators, which can be transformed into the frequency domain, can generally only provide Volterra modelling and analysis in the frequency-domain over a fraction of the entire framework of weak nonlinearity. This paper discusses the problem of using a new non-parametric routine to extend the capability of Volterra analysis, in the frequency domain, to weakly nonlinear Duffing systems at a wider range of excitation amplitude range which the current underlying nonlinear differential equation models fail to address.

**Keywords:** Volterra series**,** GFRF's**,** non-parametric methods

## 1 Introduction

The Volterra series, associated with so-called weakly nonlinear systems, is a direct generalisation of the linear convolution integral and has been very useful in the representation, analysis and design of nonlinear systems, both in the time and the frequency domain. For the last few decades, Volterra theory has been extensively studied. Summaries of the major contributions can be found in Schetzen(1980), Billings (1980), Rugh(1981) , Sandberg(1984), Doyle III, *et al*, (2002).

Based on the Volterra series representation, Generalised Frequency Response Functions (GFRF's) provide an intuitive representation of nonlinear systems in the frequency-domain, similar to the Frequency Response Function for linear systems. Many nonlinear phenomena can be interpreted using the GFRF's. Most of the applications of Volterra theory are found in the field of mechanical engineering and electrical engineering, where the well-known Duffing system is among the most extensively studied.

The Duffing oscillator, described by a cubic nonlinear differential equation, can be transformed into the frequency-domain to obtain the GFRF's. The resulting GFRF's, however, are only valid in providing the Volterra representation in the frequency-domain within a certain region of excitation amplitude and therefore will generally provide limited capacity in performing any frequency-domain analysis. In this paper a

new non-parametric method is proposed to construct piecewise GFRF's within the framework of weak nonlinearity but outside the convergence radius of the original Duffing model. Consequently, the new results extend the well used results based on weakly nonlinear effects to apply to a much broader class of nonlinear systems.

This paper is organised as follows. In section 2 the Volterra/frequency modelling for Duffing oscillators is reviewed and forms the basis of the results in the later sections. In section 3, the new method is presented. In section 4, a numerical example is used to compare the new method with the parametric method and to demonstrate the application of the new method, and finally in section 5 conclusions are given.

## 2 Volterra modelling for nonlinear systems in the time and frequency domain

Consider a symmetric Duffing oscillator, with cubic nonlinearity, subject to a sinusoidal excitation as

$$m\ddot{y}(t) + c\dot{y}(t) + k_1 y(t) + k_3 y^3(t) = u(t) \tag{1}$$

where $u(t) = A\cos(\omega t)$ and $m, c, k_1$ and $k_3$ are the mass, the damping, the linear stiffness and nonlinear stiffness respectively.

System (1) can be defined by the nonlinear mapping

$$y(t) = \mathbf{T}[u(t)] \tag{2}$$

In the framework of weak nonlinearity, (2) can be further described by Volterra(1930) series modelling as

$$y(t) = \sum_{n=1}^{\infty} y_n(t) \tag{3.a}$$

and $y_n(t)$ is the '*n*-th order output' of the system

$$y_n(t) = \mathbf{T}_n[u(t)] = \int \cdots \int h_n(\tau_1, \cdots \tau_n) \prod_{i=1}^{n} u(t-\tau_i) d\tau_i \qquad n > 0 \tag{3.b}$$

where $T_n[\cdot]$ is called the '*n*th-order Volterra operator', and $h_n(\tau_1, \cdots, \tau_n)$ is called the '*n*th-order kernel' or 'nth-order impulse response function'. If *n=1*, this reduces to the familiar linear convolution integral. In this sense, the Volterra model is a direct generalisation of the linear convolution integral, therefore providing an intuitive representation in a simple and easy to apply way.

A valid Volterra series representation means valid Generalised Frequency Response Functions(GFRF's) exist. The GFRF's are obtained by taking the multi-dimensional Fourier transform of $h_n(\cdot)$:

$$H_n(\omega_1, \cdots, \omega_n) = \int_{-\infty}^{\infty} \cdots \int_{-\infty}^{\infty} h_n(\tau_1, \cdots, \tau_n) \exp(-j(\omega_1 \tau_1 + \cdots + \omega_n \tau_n)) d\tau_1 \cdots d\tau_n \tag{4}$$

The generalised frequency response functions have proved to be an important analysis and design tool for characterising nonlinear phenomena. For the nonlinear differential equation (1), the GFRF's can be obtained by mapping (1) into the frequency-domain using the probing method (Billings and Peyton Jones, 1990). Because (1) has only an odd order nonlinearity in the response, the even order GFRF's are equal to zero. Therefore the first 3 orders of GFRF's for (1) can be expressed as

$$H_1(s)\big|_{s=j\omega} = \frac{1}{ms^2 + cs + k_1}, \qquad H_2(s_1, s_2)\big|_{\substack{s_1 = j\omega_1 \\ s_2 = j\omega_2}} = 0$$
$$H_3(s_1, s_2, s_3)\big|_{\substack{s_1 = j\omega_1 \\ s_2 = j\omega_2 \\ s_3 = j\omega_3}} = -k_3 H_1(s_1) H_1(s_2) H_1(s_3) H_1(s_1 + s_2 + s_3) \tag{5}$$

The discrete time domain counterpart of the continuous time domain SISO Volterra expression (3) is

$$y(k) = \sum_{n=1}^{\infty} y_n(k) \tag{6.a}$$

where

$$y_n(k) = \sum_{-\infty}^{\infty} \cdots \sum_{-\infty}^{\infty} h_n(\tau_1, \cdots, \tau_n) \prod_{i=1}^{n} u(k - \tau_i) \qquad n > 0, k \in \mathrm{Z} \tag{6.b}$$

In practice only the first few kernels are used on the assumption that the contribution of the higher order kernels falls off rapidly. A weakly nonlinear system means that the systems can be adequately represented by a Volterra series with just a few terms, in which cases truncated versions of (3) and (6) are adopted. A truncated discrete time Volterra series is also called a NX (Nonlinear model with eXogenous inputs) model.

In practice, nonlinear system identification in the frequency-domain to determine the GFRF's, involves using parametric or non-parametric estimation methods. The parametric method involves fitting a parametric discrete time model, e.g., NARX or NX model, and then mapping this into the frequency-domain (Peyton Jones and Billings, 1989). Traditionally the non-parametric method involves estimating the GFRF's using extensions of traditional spectral analysis based on the frequency-domain Volterra model (Kim and Powers, 1988; Nam and Powers, 1994). Recently a new non-parametric method was proposed using the time-domain excitation-response samples directly (Li and Billings, 2010b) and hence avoiding all the computations associated with Fourier based methods. In the following sections, this new non-parametric method is improved to accommodate the Volterra modelling in the frequency-domain for the excitation range where the original GFRF's in (5) from the underlying system (1) fail. This means that the analysis procedure can be consequently extended to apply to a much broader class of systems and nonlinear behaviours. The advantage of the new non-parametric method versus the parametric method is also discussed.

## 3 Estimation of GFRF's for Duffing oscillators over different ranges of excitation amplitude

The ideal situation is that the GFRF's in (5) can provide important analysis in the frequency-domain over the whole weak nonlinearity range. However, this is not true in general. A number of criteria have been proposed for the estimation of the upper limit of the excitation amplitude so that the GFRF's in (5) can provide a valid Volterra representation (Tomlinson, *et al*, 1996; Peng and Lang, 2007;Li and Billings, 2010a).

The upper limits revealed by the above criteria are, however, not the overall upper boundary of the weak nonlinearity of a Duffing oscillator, but the boundary that underlying differential equation model can provide in terms of Volterra analysis. In fact for many Duffing systems the GFRF's from the underlying differential equation model may only cover a small part of the weakly nonlinear region, and the objective of this study is to construct the GFRF's for the under-represented region.

Assume that the sinusoidal excitation is

$$u(t) = A\cos(\omega t) = \frac{A}{2}e^{j\omega t} + \frac{A}{2}e^{-j\omega t} \tag{7}$$

with $A \in (AL, AU)$ where $AL, AU$ represent the lower and upper limits of an amplitude range where the weakly nonlinear system can not be analyzed by the GFRF's derived from the underlying system model. Further assume that the weakly nonlinear oscillator for the amplitude range $A \in (AL, AU)$ can be expressed by the first three Volterra kernels. Then the first order response $y_1(t)$ can be derived by (Schetzen, 1980)

$$\begin{aligned} y_1(t) &= \int_{-\infty}^{\infty} \tilde{h}_1(\tau)u(t-\tau)d\tau \\ &= \frac{A}{2}\tilde{H}_1(\omega)e^{j\omega t} + \frac{A}{2}\tilde{H}_1(-\omega)e^{-j\omega t} \\ &= AR_1\cos(\omega t) - AI_1\sin(\omega t) \end{aligned} \tag{8}$$

where $\tilde{H}_1(\omega) = R_1(\omega) + jI_1(\omega)$.

Similarly the third order response $y_3(t)$ can be determined as

$$\begin{aligned} y_3(t) &= \int_{-\infty}^{\infty}\int_{-\infty}^{\infty}\int_{-\infty}^{\infty} \tilde{h}_3(\tau_1,\tau_2,\tau_3)u(t-\tau_1)u(t-\tau_2)u(t-\tau_3)d\tau_1 d\tau_2 d\tau_3 \\ &= 2(\frac{A}{2})^3 \operatorname{Re}\{\tilde{H}_3(\omega,\omega,\omega)e^{j3\omega t}\} + 6(\frac{A}{2})^3 \operatorname{Re}\{\tilde{H}_3(\omega,\omega,-\omega)e^{j\omega t}\} \\ &= 2(\frac{A}{2})^3 R_3\cos(3\omega t) - 2(\frac{A}{2})^3 I_3\sin(3\omega t) \\ &\quad + 6(\frac{A}{2})^3 R_{31}]\cos(\omega t) - 6(\frac{A}{2})^3 I_{31} - \sin(\omega t) \end{aligned} \tag{9}$$

where $\tilde{H}_3(\omega,\omega,\omega) = R_3(\omega,\omega,\omega) + jI_3(\omega,\omega,\omega)$ and $\tilde{H}_3(\omega,\omega,-\omega) = R_{31}(\omega,\omega,-\omega) + jI_{31}(\omega,\omega,-\omega)$.

The overall expression of the response using the first three Volterra kernel terms, by combining (8) and (9), is given as

$$\begin{aligned} y(t) &= y_1(t) + y_3(t) + e(t) \\ &= [AR_1 + 6(\frac{A}{2})^3 R_{31}]\cos(\omega t) + [AI_1 + 6(\frac{A}{2})^3 I_{31}][-\sin(\omega t)] \\ &\quad + 2(\frac{A}{2})^3 R_3\cos(3\omega t) + 2(\frac{A}{2})^3 I_3[-\sin(3\omega t] + e(t) \end{aligned} \tag{10}$$

where $e(t)$ represents the truncation error.

When the system (1) is simulated the excitation-response can be collected at sampling intervals at $t = kT$, $k = 1,2,\cdots,N$, then equation (10) can be expressed in a discrete time format as

$$
\begin{aligned}
y(k) &= [AR_1 + 6(\frac{A}{2})^3 R_{31}]\cos(\omega kT) + [AI_1 + 6(\frac{A}{2})^3 I_{31}][-\sin(\omega kT)] \\
&\quad + 2(\frac{A}{2})^3 R_3 \cos(3\omega kT) + 2(\frac{A}{2})^3 I_3[-\sin(3\omega kT] + e(k) \\
&= \sum_{m=1}^{4} \theta_m p_m(k) + e(k)
\end{aligned} \tag{11}
$$

where the unknown parameters are

$$
\begin{aligned}
&\theta_1 = [AR_1 + 6(\frac{A}{2})^3 R_{31}], \quad \theta_2 = [AI_1 + 6(\frac{A}{2})^3 I_{31}] \\
&\theta_3 = R_3, \qquad\qquad\qquad \theta_4 = I_3
\end{aligned} \tag{12}
$$

and the regressors are

$$
\begin{aligned}
&p_1(k) = \cos(\omega kT), \quad p_2(k) = -\sin(\omega kT) \\
&p_3(k) = 2(\frac{A}{2})^3 \cos(3\omega kT), \quad p_4(k) = -2(\frac{A}{2})^3 \sin(3\omega kT)
\end{aligned} \tag{13}
$$

The unknown parameters $\theta^T = [\theta_1 \ \theta_2 \ \theta_3 \ \theta_4]$ can be estimated from (11) using a standard Least Square(LS) method.

It is assumed that $\tilde{H}_1$ and $\tilde{H}_3$ remain invariant over a certain amplitude range $A \in (AL, AU)$, then the constant estimates $\hat{R}_1$, $\hat{R}_{31}$ and $\hat{I}_1$, $\hat{I}_{31}$ can be separated from the estimates of $\hat{\theta}_1$ and $\hat{\theta}_2$ in (12) by the following procedure.

Setting the excitation amplitude

$$A^i, \quad i = 1,2,\cdots M$$

and collecting $M$ Least Square estimates of $\hat{\theta}_1^i$ and $\hat{\theta}_2^i$, $\quad i = 1,2,\cdots M$ from (11) to form

$$\hat{\boldsymbol{\theta}}_1 = \mathrm{P} * R \tag{14a}$$

and

$$\hat{\boldsymbol{\theta}}_2 = \mathrm{P} * I \tag{14b}$$

where

$$
\begin{aligned}
&\hat{\boldsymbol{\theta}}_1 = [\hat{\theta}_1^1 \quad \hat{\theta}_1^2 \quad \cdots \hat{\theta}_1^M]^T \\
&\hat{\boldsymbol{\theta}}_2 = [\hat{\theta}_2^1 \quad \hat{\theta}_2^2 \quad \cdots \hat{\theta}_2^M]^T \\
&R = [R_1 \quad R_{31}] \\
&I = [I_1 \quad I_{31}]
\end{aligned}
$$

$$\mathrm{P}=\begin{bmatrix} A^{1} & 6(\frac{\mathrm{A}^{1}}{2})^{3} \\ A^{2} & 6(\frac{\mathrm{A}^{2}}{2})^{3} \\ \vdots & \vdots \\ A^{M} & 6(\frac{\mathrm{A}^{\mathrm{M}}}{2})^{3} \end{bmatrix}$$

The standard Least Square method can be applied to (14) to obtain

$$\begin{aligned} \hat{R} &= [\hat{R}_1 \ \hat{R}_{31}] = (\mathrm{P}^T\mathrm{P})^{-1}P^T\hat{\boldsymbol{\theta}}_1 \\ \hat{I} &= [\hat{I}_1 \ \hat{I}_{31}] = (\mathrm{P}^T\mathrm{P})^{-1}P^T\hat{\boldsymbol{\theta}}_2 \end{aligned} \tag{15}$$

The estimates of $\hat{R}_3$ and $\hat{I}_3$ can then be obtained by

$$\hat{R}_3 = \frac{\sum_{i=1}^{M}\hat{\theta}_3^i}{M} \qquad \text{and} \qquad \hat{I}_3 = \frac{\sum_{i=1}^{M}\hat{\theta}_4^i}{M} \tag{16}$$

The co-ordination of the fixed $\hat{R}$ and $\hat{I}$ in (14)—(15) plays the key role in the satisfactory approximation of first order harmonic components in the response over the specified amplitude range as in (11). Apart from the estimation of the GFRF's, other essential information is the significance of the nonlinearity. One way of doing this is to use a new method to calculate the relative contribution of each order of kernel in the response in terms of energy, which can be done using the following orthogonalization procedure.

Consider a signal that consists of a number of components as

$$y = \sum_{i=1}^{K}\rho_i + e \tag{17}$$

where $e$ is the modelling error.

An auxiliary model of (17) can be constructed as

$$y = \sum_{i=1}^{K} g_i w_i + e \tag{18}$$

where $w_i, i = 1, \cdots, K$ satisfy the orthogonal property as

$$w_i^T w_j = 0, i \neq j \tag{19}$$

The orthogonalization procedure from (17) to (19) can be constructed using, for example, the classical Gram-Schmidt method (Björck, 1967).

Therefore from (18) the energy of $y$ can be expressed as

$$y^T y = \sum_{i=1}^{K} g_i^2 w_i^T w_i + e^T e \tag{20}$$

The energy contribution of the individual component can be defined in percentage as

$$E_i = \frac{g_i^2 w_i^T w_i}{y^T y} \times 100 \tag{21}$$

Now back to our problem. Once the estimates of the GFRF's of (1) over a certain amplitude range $A \in (AL, AU)$ are obtained using the procedure (11)—(16), the response at the particular excitation amplitude $A^i$ can be re-arranged with respect to contributors of each order to the GFRF as

$$\begin{aligned} y^i(k) &= \hat{y}^i(k) + e^i(k) \\ &= \underbrace{A^i \hat{R}_1 \cos(\omega k T) - A^i \hat{I}_1 \sin(\omega k T)}_{Contribution\ by\ \tilde{H}_1(\omega)} + \underbrace{6(\frac{A^i}{2})^3 \hat{R}_{31} \cos(\omega k T) - 6(\frac{A^i}{2})^3 \hat{I}_{31} \sin(\omega k T)}_{Contribution\ by\ \tilde{H}_3(\omega,\omega,-\omega)} \\ &\quad + \underbrace{2(\frac{A^i}{2})^3 \hat{R}_3 \cos(3\omega k T) - 2(\frac{A^i}{2})^3 \hat{I}_3 \sin(3\omega k T}_{Contribution\ by\ \tilde{H}_3(\omega,\omega,\omega)} + e^i(k) \end{aligned} \tag{22}$$

It is not possible to compute the energy contribution of individual real and imaginary parts of each order of GFRF's because both the real part of $\tilde{H}_1(\omega)$, $\hat{R}_1$, and $\tilde{H}_3(\omega,\omega,-\omega)$, $\hat{R}_{31}$, relate to the same sinusoidal component $\cos(\omega k T)$. It is the same situation for the imaginary part of $\tilde{H}_1(\omega)$ and $\tilde{H}_3(\omega,\omega,-\omega)$. A direct employment of the orthogonalization procedure in (17)—(20) to (22) will result in a singularity problem. Thus (22) needs to be further wrapped as

$$\begin{aligned} y^i(k) &= \hat{y}^i(k) + e(k) \\ &= \underbrace{A^i \sqrt{\hat{R}_i^2 + \hat{I}_i^2}\, \sin[\omega k T - \mathrm{atan}(\tfrac{\hat{R}_i}{\hat{I}_i})]}_{Contribution\ by\ \tilde{H}_1(\omega)} + \underbrace{6(\frac{A^i}{2})^3 \sqrt{\hat{R}_{31}^2 + \hat{I}_{31}^2}\, \sin[\omega k T - \mathrm{atan}(\tfrac{\hat{R}_{31}}{\hat{I}_{31}})]}_{Contribution\ by\ \tilde{H}_3(\omega,\omega,-\omega)} \\ &\quad + \underbrace{2(\frac{A^i}{2})^3 \sqrt{\hat{R}_3^2 + \hat{I}_3^2}\, \sin[\omega k T - \mathrm{atan}(\tfrac{\hat{R}_3}{\hat{I}_3})]}_{Contribution\ by\ \tilde{H}_3(\omega,\omega,\omega)} + e(k) \\ &= \sum_{i=1}^{3} \rho_i(k) + e(k) \end{aligned} \tag{23}$$

where

$$\rho_1 = A^i \sqrt{\hat{R}_i^2 + \hat{I}_i^2}\, \sin[\omega k T - \text{atan}(\tfrac{\hat{R}_i}{\hat{I}_i})]$$

$$\rho_2 = 6(\frac{A^i}{2})^3 \sqrt{\hat{R}_{31}^2 + \hat{I}_{31}^2}\, \sin[\omega k T - \text{atan}(\tfrac{\hat{R}_{31}}{\hat{I}_{31}})] \tag{24}$$

$$\rho_3 = 2(\frac{A^i}{2})^3 \sqrt{\hat{R}_3^2 + \hat{I}_3^2}\, \sin[\omega k T - \text{atan}(\tfrac{\hat{R}_3}{\hat{I}_3})]$$

The energy contributions of each term $\rho_i$ which corresponds to the relevant kernels can now be derived using the orthogonalization procedure described in (17)—(20).

By repeating the procedure (7)—(16) over each segment of the excitation amplitude range where the GFRF's can be approximately considered invariant, piecewise GFRF's for the whole range of interest can be constructed. The size of each amplitude segment is determined basically upon the accuracy requirement. The smaller the size of the segment the smaller the truncation errors over this segment. For qualitative analysis purpose, the size can be accordingly stretched.

## 4 Numerical illustrations and analysis

The coefficients of the Duffing oscillator used in the numerical study are

$$m = 1, c = 0.2, k_1 = 1, k_3 = 0.5 \tag{25}$$

The GFRF's for the underlying system (25) can be computed using (5) and are given in Table 1.

| | |
|---|---|
| $H_1(\omega)$ | -0.5125 - 0.0922 $j$ |
| $H_3(\omega, \omega, -\omega)$ | 0.0044+0.0016 $j$ |
| $H_3(\omega, \omega, \omega)$ | -4.2792e-05- 3.1797e-05 $j$ |

**Table 1. The GFRF's from the original system (25) at** $\omega = 1.7\ rad/\sec$

Li and Billings (2010a) show that the upper limit of a valid Volterra series representation by the original GFRF's in Table 1 can be given in terms of the $H_1(\omega)$ and the nonlinear coefficients $k_3$ as

$$A_L(\omega) = 2 \Big/ [\sqrt{|k_3|}(3|H_1(\omega)|)^{3/2}] \tag{26}$$

The response diagram of system (25) excited at $\omega = 1.7$ rad/sec is shown in Figure 1, together with the upper limit point $A_L(\omega)\big|_{\omega=1.7} = 1.4485$.

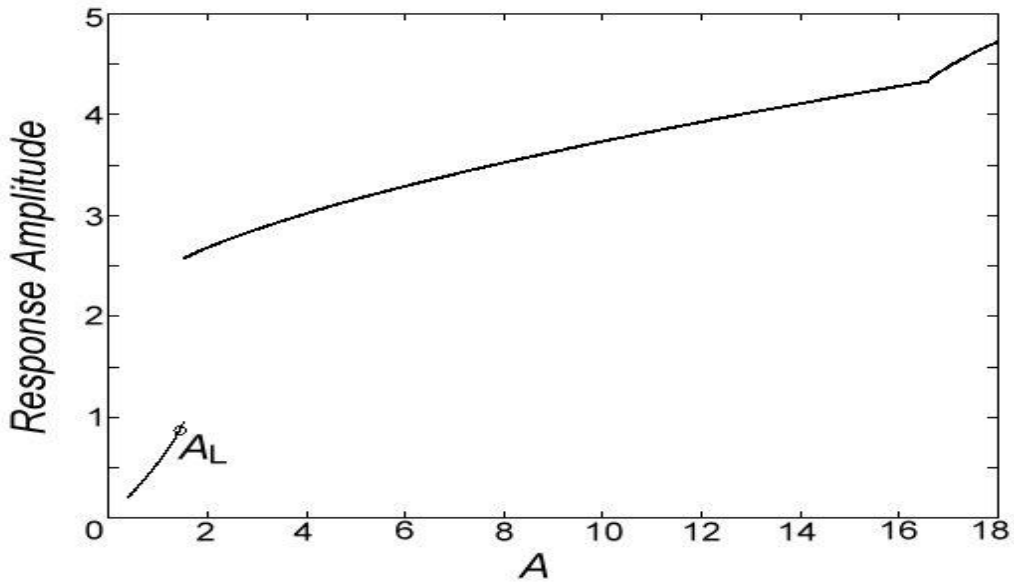


**Figure 1. The response diagram of system (25) at $\omega = 1.7$ rad/sec**

It is very clear that as the excitation amplitude increases to around $A$=1.5, a discontinuity in the response amplitude occurs. The criterion (26) can very accurately predict this discontinuity, and its implication suggests that this is the upper limit below which the original GFRF's in (5) can be expected to provide a valid Volterra representation/analysis. Due to the analytic nature of the Volterra series representation, the GFRF's in (5) can no longer provide a valid frequency-domain representation and analysis after this jump at around $A$=1.5.

To gain insight into the dynamics of system (25) (Aguirre and Billings, 1995a,1995b) in the frequency-domain, a response spectrum map(RSM) (Billings and Boaghe, 2001), which can be considered as the frequency-domain counterpart of the bifurcation diagram and in this case the response diagram in Figure 1, is produced in Figure 2.

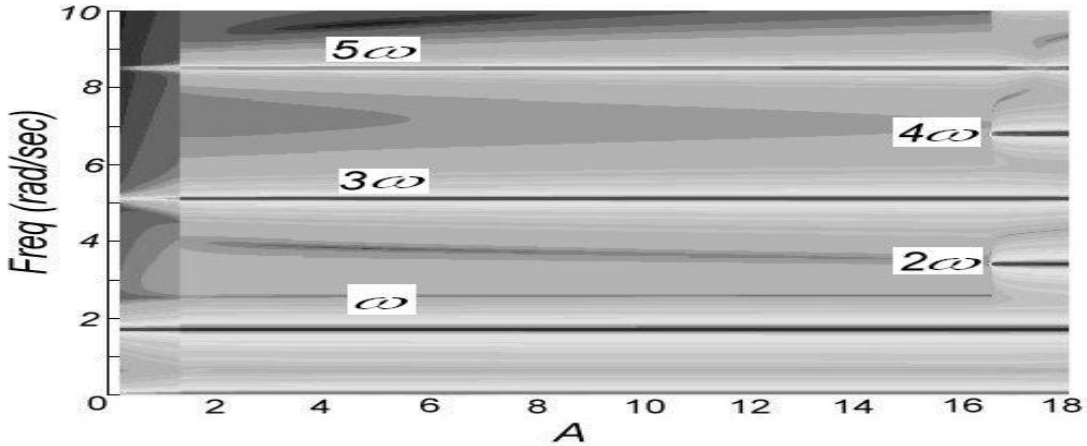


**Figure 2. The response spectrum map of system (25) at $\omega = 1.7$ rad/sec**

An inspection of Figure 2 reveals that for the excitation range after the jump, that is $1.5<A<16.6$, the frequency components in the response remain the same, an important characteristic of weak nonlinearity. This suggests that there could be a valid Volterra representation during this range. It also implies that the GFRF's in (5) by the original system (25) can only provide a Volterra representation/analysis over a fraction of the whole weakly nonlinear range. The object of the present study is to find out the unknown GFRF's for the amplitude range $1.5<A<16.6$.

As mentioned in Section 2 there are generally two classes of methods for estimating the GFRF's out of excitation-response measurements, the parametric and the non-parametric methods. Both methods work very well for the excitation amplitude range before the jump. However, as the amplitude increases above the jump point, the situation changes. To show this, select the first segment of the excitation amplitude range as $A^{(1)} \in (1.5, 2.6)$. First, the capacity of the parametric method is investigated. The system (25) was excited at the excitation amplitude $A$=2.1 and frequency $\omega = 1.7\ rad/\sec$. A parametric NX model can be fitted using the collected response-excitation data set as

$$\begin{aligned} y(k) = {} & 3.1869\, u(k-3) - 2.1204\, u(k-2) + 0.27892\, u^3(k-3) \\ & - 0.23795\, u(k-2)u^2(k-3) \end{aligned} \tag{27}$$

The GFRF's can be obtained by mapping the nonlinear difference model (27) into frequency-domain (Peyton Jones and Billings, 1989), shown in Table 2.

| | |
|---|---|
| $\tilde{H}_1(\omega)$ | 0.9870 - 0.4654$j$ |
| $\tilde{H}_3(\omega,\omega,-\omega)$ | 0.0386 - 0.0179$j$ |
| $\tilde{H}_3(\omega,\omega,\omega)$ | 0.0140 - 0.0448$j$ |

**Table 2. GFRF's by NX model (27) at** $\omega = 1.7\ rad/\sec$

A clear numerical measure of the closeness of fit between the synthesized response and the real response can be obtained by using the Normalised Root Mean Square Error defined as

$$NRMSE = \sqrt{\frac{\sum (y_{real}(k) - \hat{y}(k))^2}{\sum (y_{real}(k) - y_{mean}(k))^2}} \tag{28}$$

where $\hat{y}(k)$ is the synthesized response using (11) with the GFRF's in Table 1, $y_{real}(k)$ is the real response and $y_{mean}(k)$ is the mean value of the real data set $y_{real}(k)$. Figure 3 (dashed line) shows the *NRMSE* along the $A^{(1)} \in (1.5,2.6)$. It is very clear from Figure 3 that the GFRF's from (27) can provide an extremely accurate representation at the excitation amplitude point $A$=2.1, but the *NRMSE* quickly

becomes unacceptable as the amplitude moves away from $A$=2.1. This suggests that the GFRF's obtained from the parametric modelling is amplitude-variant, so in order to obtain a desired GFRF coverage for the whole segment $A^{(1)} \in (1.5,2.6)$, a large amount of parametric models, similar to the one in (27), have to be fitted at each amplitude point. This is of course a significant inconvenience from the application point of view.

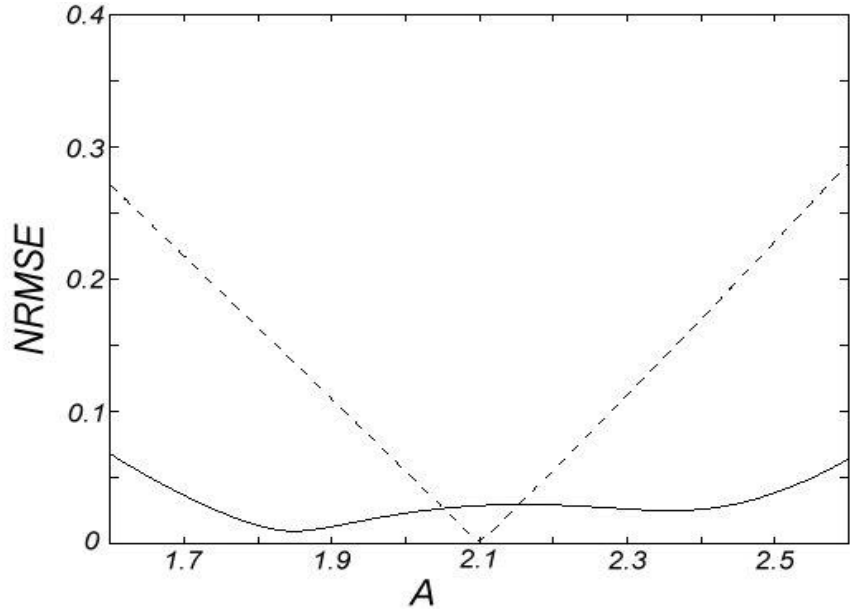


**Figure 3. The *NRMSE*: dashed—parametric result using GFRF's from Table 1 and Solid—non-parametric result using GFRF's from Table 2.**

Now assuming that the GFRF's are amplitude-invariant within $A^{(1)} \in (1.5,2.6)$, and the new non-parametric procedure introduced in Section 3 is applied. The estimated constant GFRF's for the whole segment $A^{(1)} \in (1.5,2.6)$ are given in Table 3.

| | |
|---|---|
| $\tilde{H}_1(\omega)$ | 1.4882 - 0.9999$j$ |
| $\tilde{H}_3(\omega,\omega,-\omega)$ | -0.1087 + 0.1340$j$ |
| $\tilde{H}_3(\omega,\omega,\omega)$ | 0.0106 - 0.0495$j$ |

**Table 3. GFRF's by new non-parametric method for $A^{(1)} \in (1.5, 2.6)$ at $\omega = 1.7\ rad/\sec$**

The comparisons of synthesized response and the real response at the representative amplitudes, plotted in Figure 4, show satisfactory estimation accuracy. The *NRMSE* along the $A^{(1)} \in (1.5,2.6)$, shown in Figure 3 (Solid), remains small at all amplitude points, indicating that the fixed GFRF's in Table 2 can provide an overall representation within the whole segment.

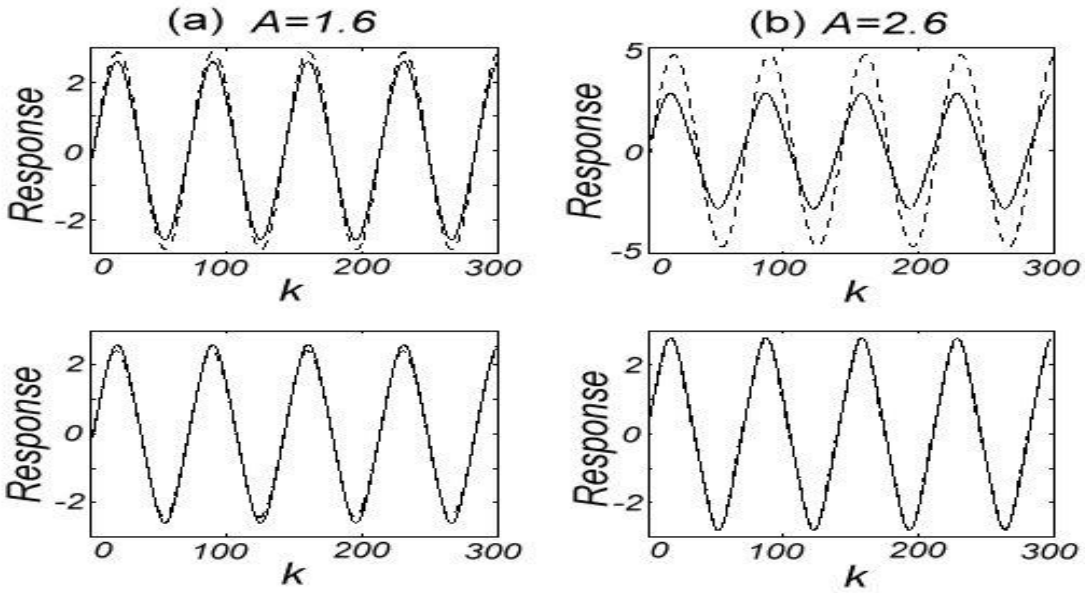


**Figure 4. Comparisons of synthesized response and the real response at (a) *A*=1.6 and (b) *A*=2.6 using the GFRF's from non-parametric method in Table 2**
**Above: synthesized up to 1st order GFRF's; Bottom: synthesized up to 3rd order GFRF's**

A repetition of the new non-parametric method over the new amplitude segments $A^{(2)} \in (2.6,4.2)$ and $A^{(3)} \in (4.2,6.6)$ produces the new piecewise GFRF's as in Tables 4 and 5.

| | |
|---|---|
| $\tilde{H}_1(\omega)$ | 1.0874 - 0.4340 $j$ |
| $\tilde{H}_3(\omega,\omega,-\omega)$ | -0.0334 + 0.0217 $j$ |
| $\tilde{H}_3(\omega,\omega,-\omega)$ | 0.0100 - 0.0116 $j$ |

**Table 4. GFRF's by new non-parametric method for $A^{(2)} \in (2.6, 4.2)$ at $\omega = 1.7\ rad/\sec$**

| | |
|---|---|
| $\tilde{H}_1(\omega)$ | 0.7649 - 0.2007 $j$ |
| $\tilde{H}_3(\omega,\omega,-\omega)$ | -0.0095 + 0.0039 $j$ |
| $\tilde{H}_3(\omega,\omega,-\omega)$ | 0.7649 - 0.2007 $j$ |

**Table 5. GFRF's by new non-parametric method for $A^{(3)} \in (4.2, 6.6)$ at $\omega = 1.7\ rad/\sec$**

This piecewise GFRF estimation procedure can be carried on until *A* reaches 16.6. The overall GFRF's, illustrated in Figure 5, shows that after a big 'jump' of the magnitudes of the GFRF's at *A*=1.5, the GFRF's gradually decrease as the excitation amplitude increases. The combined effects of decreasing GFRF's and the increasing *A*

will provide a very good prediction of the slowly increasing response amplitude as shown in Figure 1.

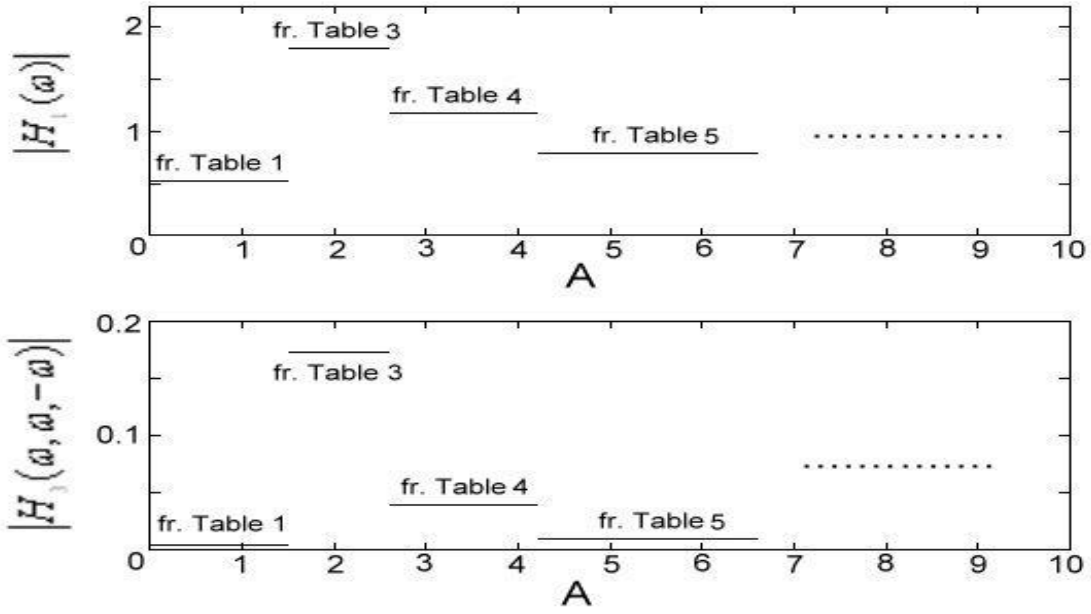


**Figure 5. The overall piecewise GFRF's**

The significance of the nonlinearity can be calculated using the procedure in (17)—(24), in terms of the energy contribution of each kernels. Table 6 compares the result before and after jump.

| | Energy Contributions ( %) | |
|---|---|---|
| | $A$=1.4 | $A$=2.1 |
| $\tilde{H}_1(\omega)$ | 99.9175 | 97.5324 |
| $\tilde{H}_3(\omega,\omega,-\omega)$ | 0.0812 | 2.2902 |
| $\tilde{H}_3(\omega,\omega,\omega)$ | 0.0013 | 0.1756 |

**Table 6. The comparison of the energy contribution before and after jump**

Table 6 gives some important information. First, the sums of the contributions by all kernels in both cases are almost 100%, indicating that up to 3rd order Volterra models are sufficient in representing the system over these ranges, and also that the estimates of the GFRF's after the jump are quite accurate. Second, the system before the jump is overwhelmingly dominated by the linear kernel, with negligible contributions from the nonlinear terms. While there is a significant increase of contribution from the cubic GFRF after the jump. Also note that there are significant changes of relative values of the GFRF's in Table 1 and 3. Both type of changes point to a fact that the jump is an increase in nonlinearity and also a significant dynamical change. However,

this change is still un-structural because after the jump the dynamic representation can still be described by the symmetric Duffing oscillator format (1) due to the same frequency components and Volterra kernels involved. The coefficients of the new asymmetric Duffing equations can be derived approximately by the following formula based on (5)

$$\begin{aligned} \hat{m} &= 1 \\ \hat{c} &= \frac{1}{\omega}\,\mathrm{Im}\left[\frac{1}{\tilde{H}_1(\omega)}\right] \\ \hat{k}_1 &= \mathrm{Re}\left[\frac{1}{\tilde{H}_1(\omega)}\right] + \omega^2 \\ \hat{k}_3 &= \frac{-\tilde{H}_3(\omega,\omega,-\omega)}{\tilde{H}_1(\omega)\tilde{H}_1(\omega)\tilde{H}_1(\omega)\tilde{H}_1(-\omega)} \end{aligned} \tag{29}$$

where the $\tilde{H}_1(\omega)$ and $\tilde{H}_3(\omega,\omega,-\omega)$ are the estimates in Table 3—5.

The symmetric Duffing oscillator expressions derived approximately from (29) over the different amplitudes segment are given as

$$\ddot{y}(t) + 0.1830\,\dot{y}(t) + 3.353\,y(t) + 0.0209\,y^3(t) = A^{(1)}\cos(\omega t) \qquad A^{(1)} \in (1.5, 2.6) \tag{30}$$

$$\ddot{y}(t) + 0.1862\,\dot{y}(t) + 3.6833\,y(t) + 0.0206\,y^3(t) = A^{(2)}\cos(\omega t) \qquad A^{(2)} \in (2.6, 4.2) \tag{31}$$

and

$$\ddot{y}(t) + 0.1880\,\dot{y}(t) + 4.113\,y(t) + 0.0240\,y^3(t) = A^{(3)}\cos(\omega t) \qquad A^{(3)} \in (4.2, 6.6) \tag{32}$$

There were significant changes in the damping, the linear stiffness and cubic nonlinear stiffness respectively before and after the jump, by comparing the true underlying system coefficients in (25) and the auxiliary model coefficients in (30)—(32), but relatively small changes in terms of mechanical dynamics after the jump between (30) to (32). These changes could provide some insights into the dynamical behaviours and supply additional information in the design and control aspects of the Duffing system over the concerned ranges.

There will be a structural dynamical change, as from Figure 2, occurring when the excitation amplitude *A* reaches 16.6, where there are both even and odd order harmonics present in the response, indicating that an asymmetric Duffing equation in a format as in (33), which has the linear, quadratic and cubic stiffness terms, is required for the system representation.

$$m'\ddot{y}(t) + c'\dot{y}(t) + k_1'y(t) + k_2'y^2(t) + k_3'y^3(t) = A'\cos(\omega t) \tag{33}$$

The identification and modelling of the latter structural change will be investigated in later studies.

## 4 Conclusions

The Volterra series representation has been widely applied in the modelling, design, analysis and control of weakly nonlinear systems. Many applications of Volterra series modelling were carried out in the frequency-domain based on the Generalised Frequency Response Functions (Worden and Manson, 2005; Tawfiq and Vinh, 2004). It is quite common that the Generalised Frequency Response Functions obtained by mapping a Duffing equation into the frequency-domain are valid only over part of the whole weakly nonlinearity framework. A new method has been developed in this paper to address the estimation of GFRF's in a piecewise manner for Duffing type oscillators for the under-represented weakly nonlinear region. In addition a new procedure to assess the energy contributions of each order kernel was introduced. The new non-parametric method has the advantage of constructing the amplitude-invariant GFRF's over a certain excitation range, avoiding building large sets of time-domain models needed by parametric methods. This makes the Volterra modelling in the frequency-domain efficient and provides a platform for the application of Volterra series theory over the region under consideration.

**Acknowledgement:** The authors gratefully acknowledge that this work was supported by the Engineering and Physical Sciences Research Council(EPSRC) UK, and a European Research Council Advanced Investigator Award.

**References:**

Aguirre, L. A. and Billings, S.A., 1995a, Retrieving dynamical invariants from chaotic data using NARMAX models, Int J Bifurcation and chaos, Vol. 5, No. 2, pp. 449-474.

Aguirre, L. A. and Billings, S.A., 1995b, Dynamical effects of overparameterization in nonlinear models, Physica D, Vol. 80,, No. 1-2, pp. 26-40.

Billings, S.A., 1980, Identification of non-linear systems—a survey, IEE Proceedings-D Control theory and applications, Vol. 127, No. 6, pp. 272-285.

Billings, S.A. and Boaghe, O.M., 2001, The response spectrum map, a frequency domain equivalent to the bifurcation diagram, Int. J. of Bifurcation and Chaos, Vol.11, No.7, pp.1961-1975.

Billings, S.A. and Peyton Jones, J.C., 1990, Mapping non-linear integro-differential equations into the frequency domain, Int.J.Control, Vol. 52, No. 4,pp.863-879.

Björck, A., 1967, Solving linear least squares problems by Gram-Schmidt orthogonalization, Nordisk Tidskr Informations-Be-handling, Vol. 7, pp. 1-21, 1967.

Doyle III, F. J., Pearson, R. K. and Ogunnaike, B. A., 2002, Identification and Control Using Volterra Models, Springer-Verlag, London .

Kim, K. I. and Powers, E. J., 1988, A digital method of modelling quadratically non-linear systems with a general random input, IEEE Transactions on Acoustics, Speech, and Signal Processing, 36, 1758-1769.

Li, L.M. and Billings, S.A., 2010a, Analysis of Nonlinear Oscillators Using Volterra Series in the Frequency Domain, to appear in the J of Sound and Vibrations.

Li, L.M. and Billings, S.A., 2010b, Estimation of Generalised Frequency Response Functions for Quadratically and Cubically Nonlinear Systems, to appear in the J of Sound and Vibrations.

Nam, S.W. and Powers, E.J., 1994, Application of Higher Order Spectral Analysis to Cubically Non-linear System Identification, IEEE Trans. on Signal Processing, Vol. 42, No.7, pp.1746-1766.

Peng, Z.K. and Lang, Z.Q., 2007, On the convergence of the Volterra-series representation of the Duffing's oscillators subjected to harmonic excitations, J. of Sound and Vibration, Vol. 305, pp.322-332.

Peyton Jones, J.C. and Billings, S.A., 1989, A Recursive algorithm for computing the frequency response of a class of non-linear difference equation models, Int. J. Control, Vol.50, No.5, pp.1925-1940.

Rugh, W.J., 1981, *Nonlinear System Theory—The Volterra/Wiener approach*, The John Hopkins University Press.

Schetzen, M., 1980, *The Volterra and Wiener Theories of Non-linear System*, New York: Wiley.

Sandberg, W., 1984, A Perspective on System Theory, IEEE Transactions on Circuits and Systems, Vol. CAS-31, No. 1, pp.88-103.

Tawfiq, I and Vinh, T, 2004, Nonlinear Behaviour of Structures Using the Volterra Series—Signal Processing and Testing Methods, Nonlinear Dynamics ,Vol. 37, No. 2, pp.129-149.

Tomlinson, G.R., Manson, G. and Lee, G.M., 1996, A simple criterion for establishing an upper limit to the harmonic excitation level of the Duffing oscillator using the Volterra Series, J. of Sound and Vibration, Vol. 190, No. 5, pp.751-762.

Worden, K. and Manson, G. , 2005, A Volterra series approximation to the coherence of the Duffing oscillator, J. of Sound and Vibration, Vol. 286, No. 3, pp. 529-547.